SUPPLEMENTAL INFORMATION

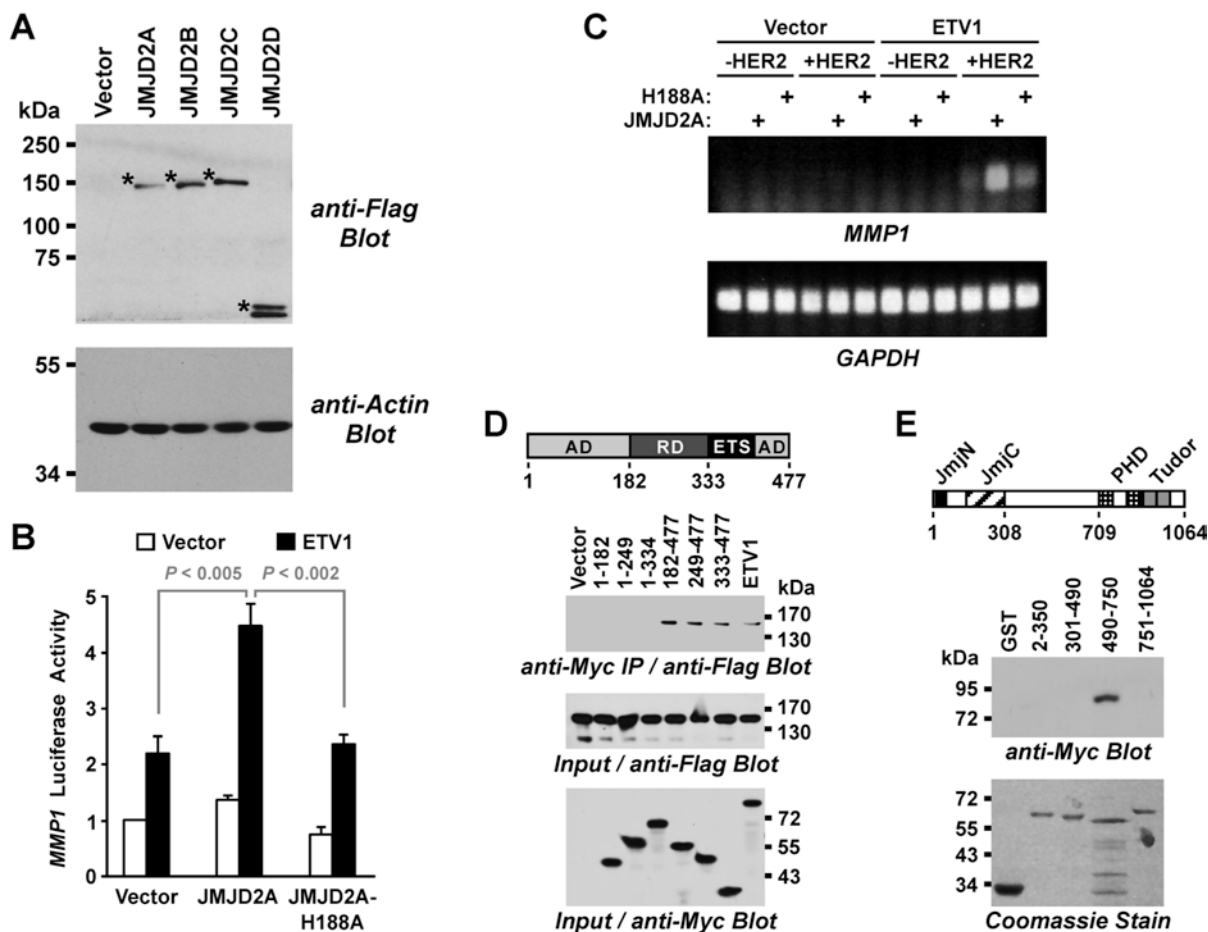# Oncogenic role of histone demethylase JMJD2A in the prostate

Tae-Dong Kim, Fang Jin, Sook Shin, Sangphil Oh, Stan A. Lightfoot, Joseph P. Grande,

Aaron J. Johnson, Jan M. van Deursen, Jonathan D. Wren, Ralf Janknecht

<u>CONTENTS</u>

**Supplemental Figure 1. JMJD2A is a cofactor of ETV1.**
(**A**) Comparable expression levels of transfected Flag-tagged JMJD2 proteins in BPH-1 cells.
(**B**) Activation of an *MMP1* luciferase reporter construct in CV-1 cells. 100 ng ETV1 expression plasmid or empty vector pEV3S, 500 ng Flag-JMJD2A expression plasmid (wild-type or H188A mutant) or pEV3S, 500 ng *MMP1* luciferase reporter plasmid, and 3.9 µg pBluescript KS$^+$ were employed for transfection of CV-1 cells (grown in 6-wells) done by the calcium phosphate coprecipitation method. Shown are averages and standard deviations (n = 3). Statistical significance was determined with Student's t-test.
(**C**) *MMP1* gene transcription in 293T cells transfected with ETV1, HER2, JMJD2A or catalytically inactive JMJD2A-H188A was measured by RT-PCR. Please note that in order to enhance *MMP1* transcription in 293T cells, ETV1 requires stimulation through the mitogen-activated protein kinase pathway, which can be achieved by overexpression of the HER2 receptor tyrosine kinase (Bosc *et al*, 2001). *GAPDH* levels were determined as a control.
(**D**) Coimmunoprecipitation assay of 293T cells transfected with 6Myc-tagged ETV1 fragments and Flag-tagged JMJD2A. Top shows a scheme of ETV1. AD, activation domain; RD, regulatory domain; ETS, DNA-binding domain.
(**E**) GST pull-down assay with indicated GST-JMJD2A fusion proteins and 6Myc-ETV1. Top shows a scheme of JMJD2A. The JmjN domain is required for catalytic activity of the JmjC domain, whereas the double PHD and Tudor domains may interact with methylated lysines.
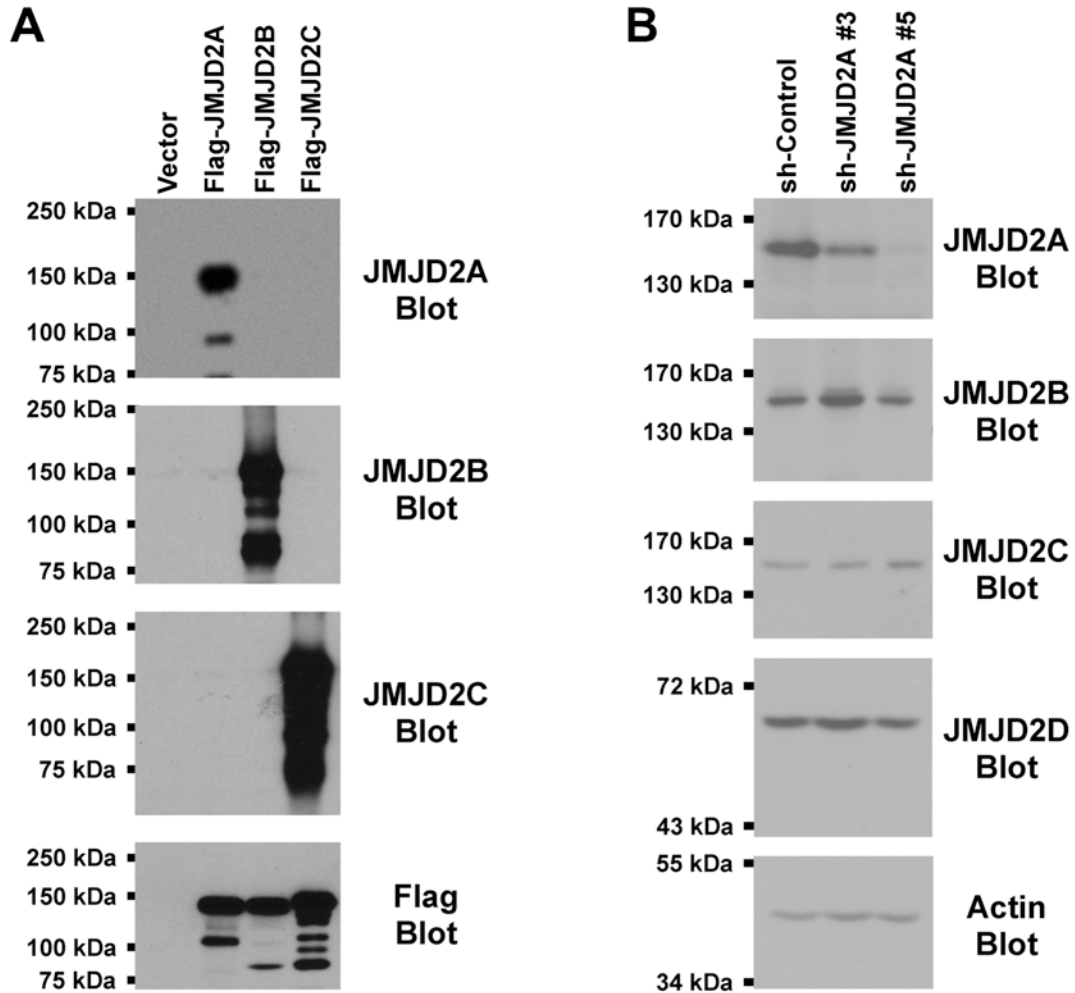
Supplemental Figure 2. Specificity of JMJD2 antibodies and JMJD2A shRNAs.
(**A**) Cell extracts derived from 293T cells transfected with indicated Flag-tagged JMJD2 proteins. JMJD2A (Bethyl A300-861A), JMJD2B (Bethyl A301-478A), JMJD2C (Bethyl A300-885A) and Flag (M2, Sigma-Aldrich F1804) antibodies were employed for western blotting. These data show that antibodies for the similarly sized JMJD2A, JMJD2B and JMJD2C proteins are specific.
(**B**) Downregulation of JMJD2A with indicated shRNAs in LNCaP cells. Western blots were probed with JMJD2A-C antibodies as in panel A, with JMJD2D antibodies (Abcam ab93694) or with actin antibodies (Sigma-Aldrich A2066). This further shows that JMJD2A antibodies are not cross-reacting with JMJD2B and JMJD2C proteins and, additionally, that JMJD2A downregulation does not cause downregulation of JMJD2B, JMJD2C or JMJD2D.
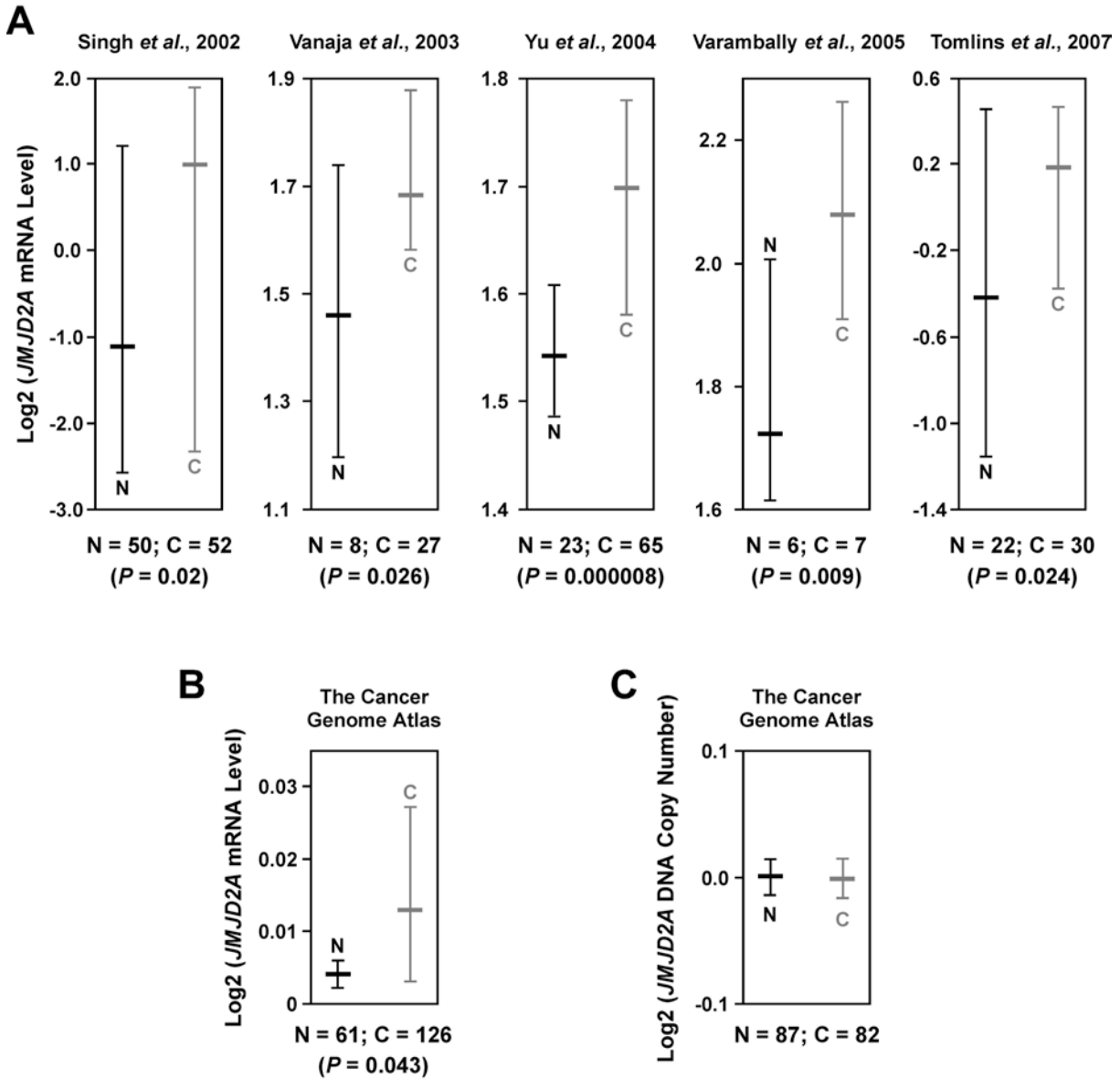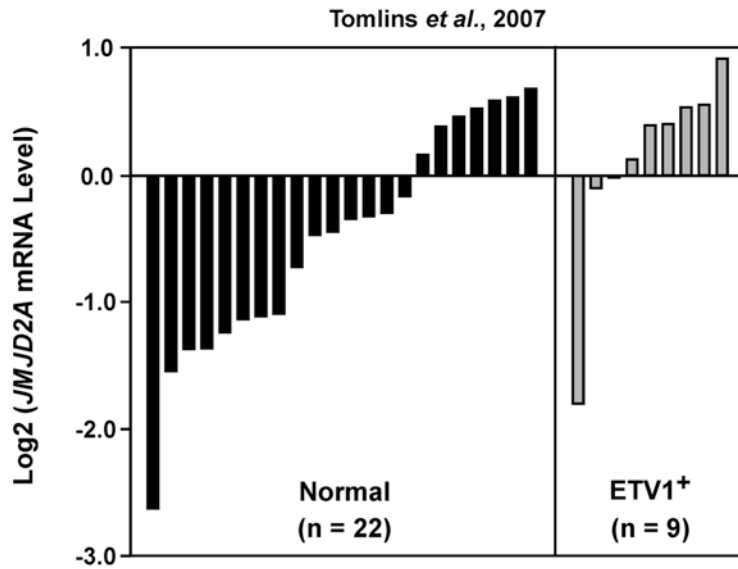
Supplemental Figure 3. Levels of *JMJD2A* in prostate tumors.
(**A**) Expression of *JMJD2A* mRNA in normal prostates ("N") and prostate carcinomas ("C"). Numbers of analyzed specimens (both for "N" and "C") are indicated below the graphs. Shown are log2-transformed mRNA levels with the median and the 25 to 75 percentile range. Statistical significance was determined with Student's t-test. Published microarray data (Singh *et al*, 2002; Vanaja *et al*, 2003; Yu *et al*, 2004; Varambally *et al*, 2005; Tomlins *et al*, 2007) were analyzed with Oncomine (www.oncomine.org).
(**B**) Analogous with data derived from *The Cancer Genome Atlas*. "N" represents normal prostates, "C" acinar prostate adenocarcinomas.
(**C**) *JMJD2A* DNA copy numbers are not significantly different between normal ("N") and cancerous ("C") prostate tissues. Data from *The Cancer Genome Atlas* were analyzed with Oncomine.

Supplemental Figure 4. High expression of *JMJD2A* in prostate tumors with an *ETV1* chromosomal translocation.

Expression of *JMJD2A* mRNA in normal prostates (n = 22) and prostate carcinomas (n = 9) characterized by a chromosomal translocation affecting the *ETV1* gene. Shown are log2-transformed mRNA levels. Each bar represents one patient. Published microarray data (Tomlins *et al*, 2007) were analyzed with Oncomine (www.oncomine.org).
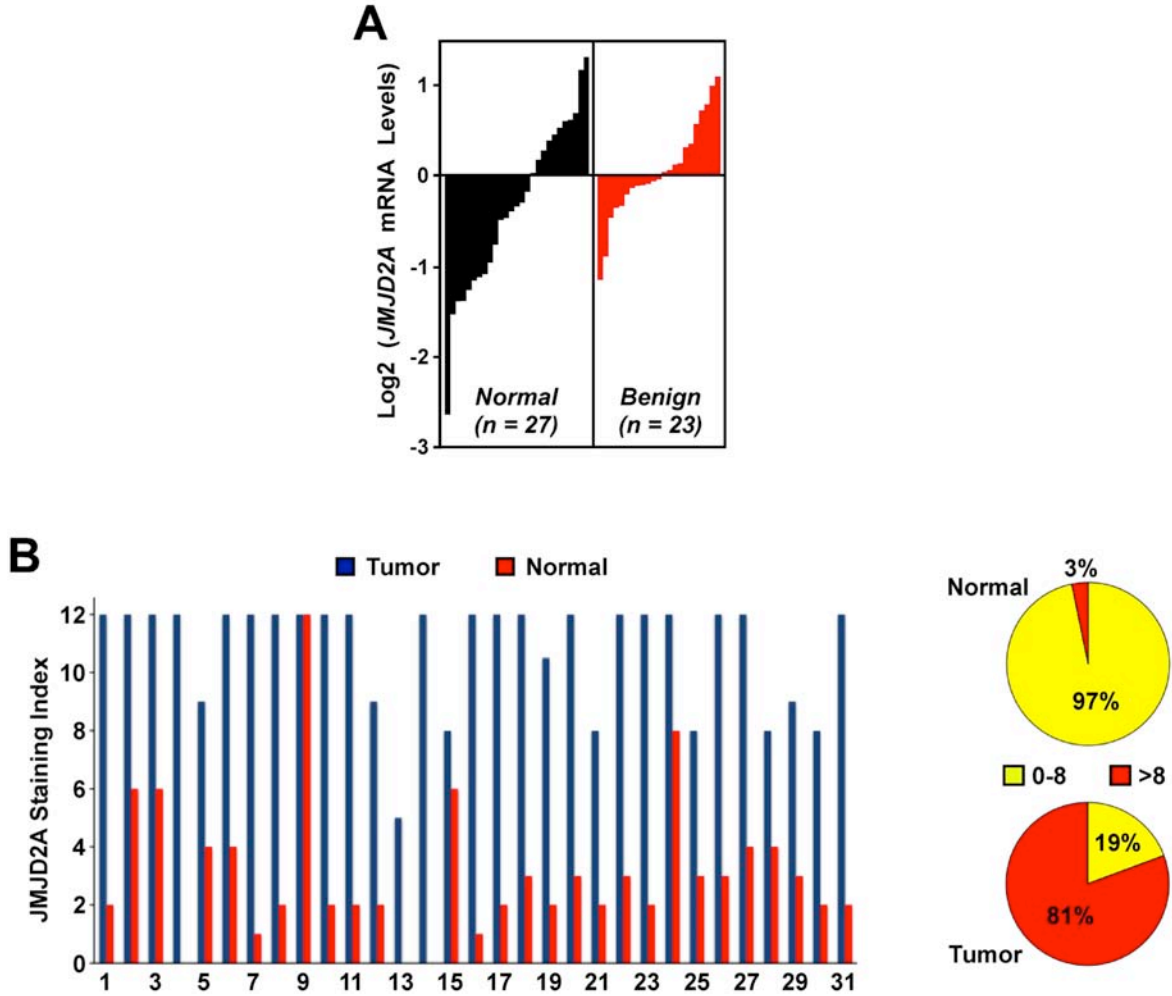
Supplemental Figure 5. Overexpression of *JMJD2A* mRNA in benign precursors of prostate tumors and nuclear staining of JMJD2A in prostate carcinomas.

(**A**) Upregulation of *JMJD2A* in benign hyperplasia and PIN *versus* normal prostate tissue (1.3-fold upregulation; P = 0.04; Student's t-test); derived from published microarray data (Tomlins *et al*, 2007) and analyzed with Oncomine (www.oncomine.org).

(**B**) Immunohistochemical nuclear staining of JMJD2A in 31 matching normal and cancerous prostate tissues (left panel). Overall, high (defined as staining index above 8) nuclear JMJD2A expression was found in 81% of tumors *versus* 3% of normal prostate tissues (right panels), which is significantly different (P = 2.2x10^{-10}; Fisher exact probability test).
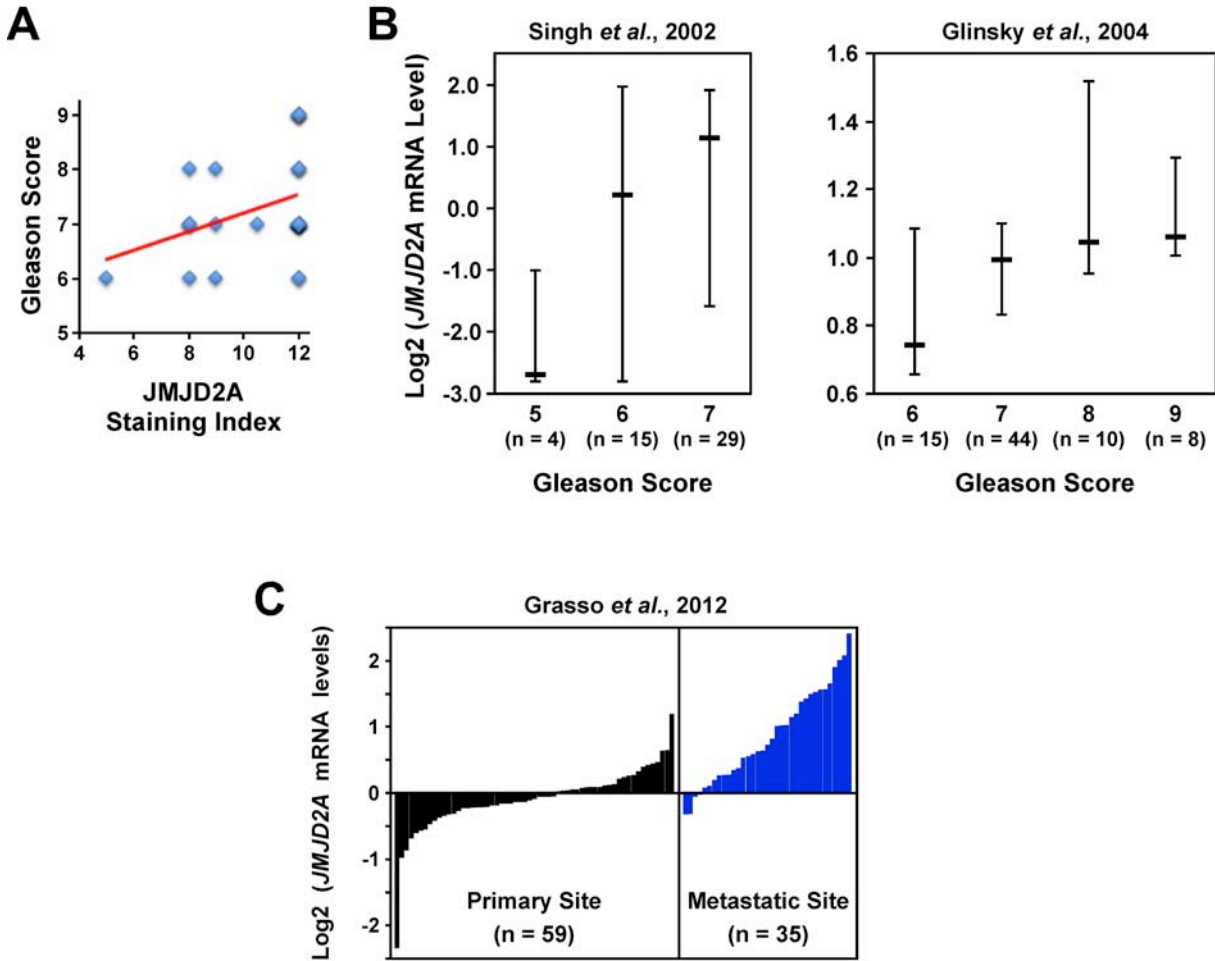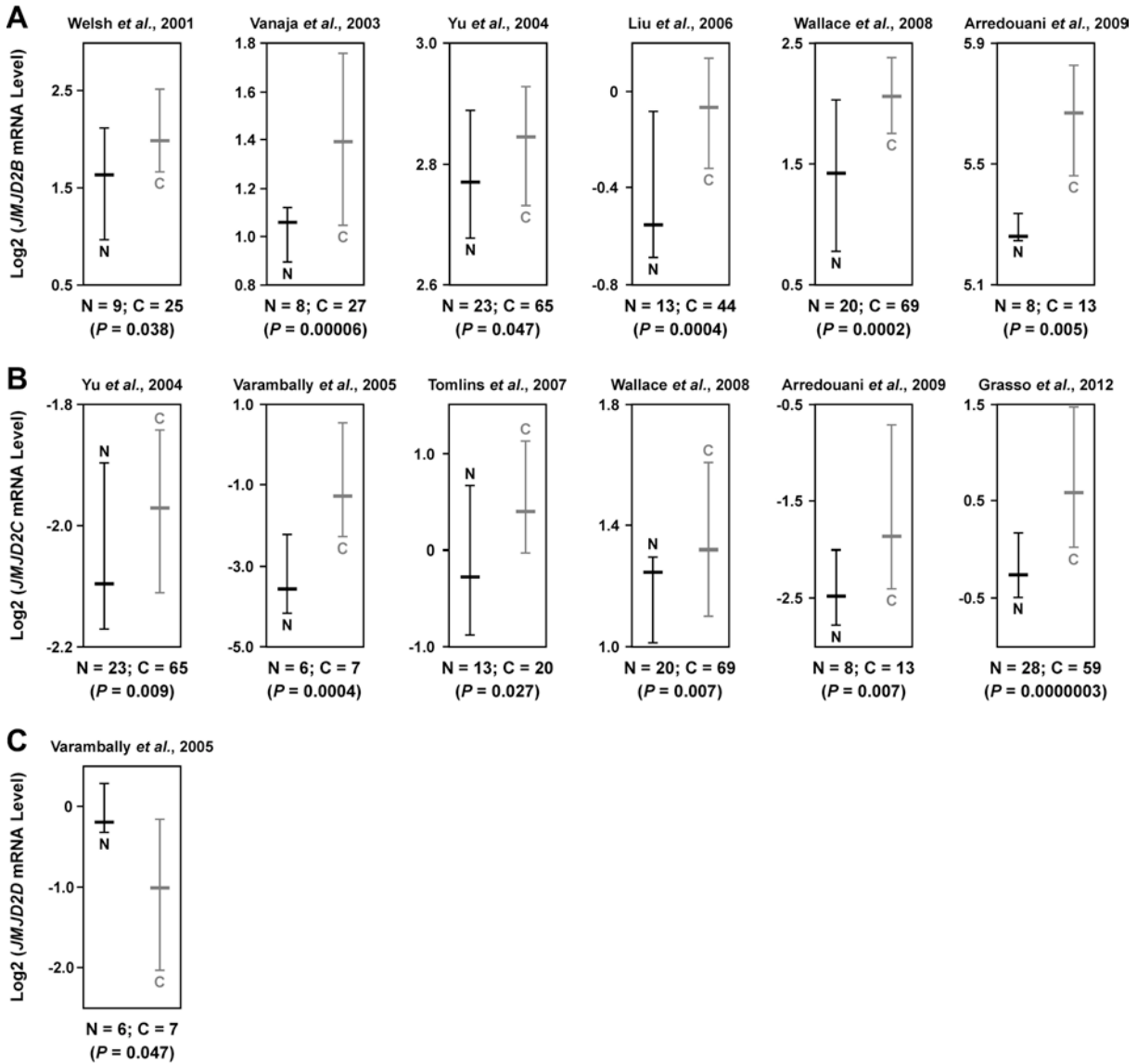
Supplemental Figure 6. JMJD2A expression is associated with Gleason score and metastasis.

(**A**) Correlation (R = 0.35, *P* = 0.028) between Gleason score and nuclear JMJD2A staining index for the 31 human prostate tumors analyzed. Trendline is marked by red color.

(**B**) Correlation between *JMJD2A* mRNA level and Gleason score in two different publicly available microarray datasets. Shown are log2-transformed mRNA levels with the median and the 25 to 75 percentile range. Statistical significance was determined with Student's t-test: *P* = 0.007 (Singh *et al*, 2002) or *P* = 0.004 (Glinsky *et al*, 2004). Data were analyzed with Oncomine (www.oncomine.org).

(**C**) Increased *JMJD2A* mRNA levels at metastatic sites compared to primary prostate tumors. Each bar represents one patient. *P* = 2.6x10^{-9} (Student's t-test); derived from published microarray data (Grasso *et al*, 2012) and analyzed with Oncomine.

Supplemental Figure 7. Levels of *JMJD2B*, *JMJD2C* and *JMJD2D* in prostate tumors.
(**A**) Expression of *JMJD2B* mRNA in normal prostates ("N") and prostate carcinomas ("C"). Numbers of analyzed specimens (both for "N" and "C") are indicated below the graphs. Shown are log2-transformed mRNA levels with the median and the 25 to 75 percentile range. Statistical significance was determined with Student's t-test. Published microarray data (Welsh *et al*, 2001; Vanaja *et al*, 2003; Yu *et al*, 2004; Liu *et al*, 2006; Wallace *et al*, 2008; Arredouani *et al*, 2009) were analyzed with Oncomine (www.oncomine.org).
(**B**) Analogous for *JMJD2C*; derived from published microarray data (Yu *et al*, 2004; Varambally *et al*, 2005; Tomlins *et al*, 2007; Wallace *et al*, 2008; Arredouani *et al*, 2009; Grasso *et al*, 2012).
(**C**) Likewise for *JMJD2D*; derived from published microarray data (Varambally *et al*, 2005).
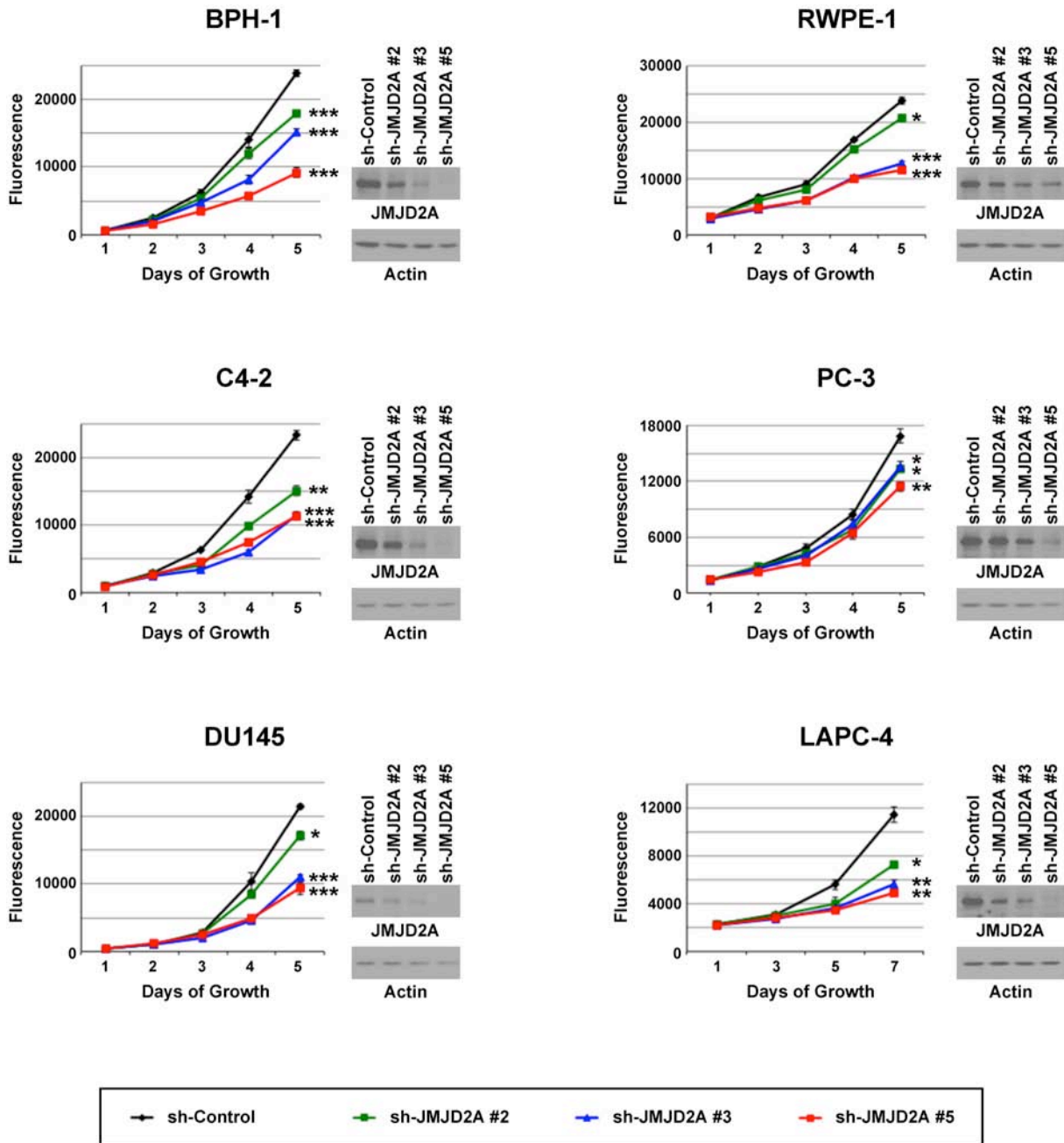
Supplemental Figure 8. Impact of JMJD2A on human prostate cell growth.
Control or three different JMJD2A shRNAs were expressed in benign (BPH-1, RWPE-1) or cancerous (C4-2, PC-3, DU145, LAPC-4) prostate cell lines. Growth was measured with the PrestoBlue fluorescence cell viability kit (Invitrogen). Averages (n = 3) with standard deviations are shown. *, $P < 0.01$; **, $P < 0.001$; ***, $P < 0.0001$ (Student's t-test). Western blots show the degree of JMJD2A and actin expression.
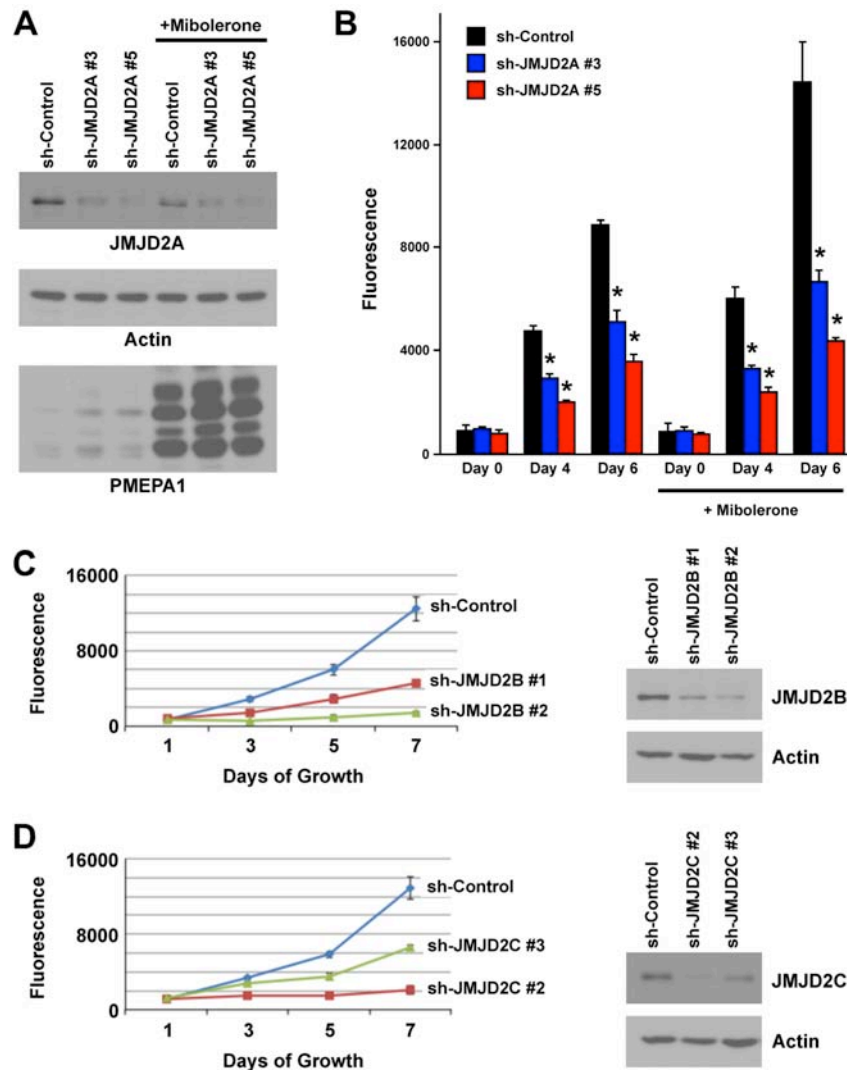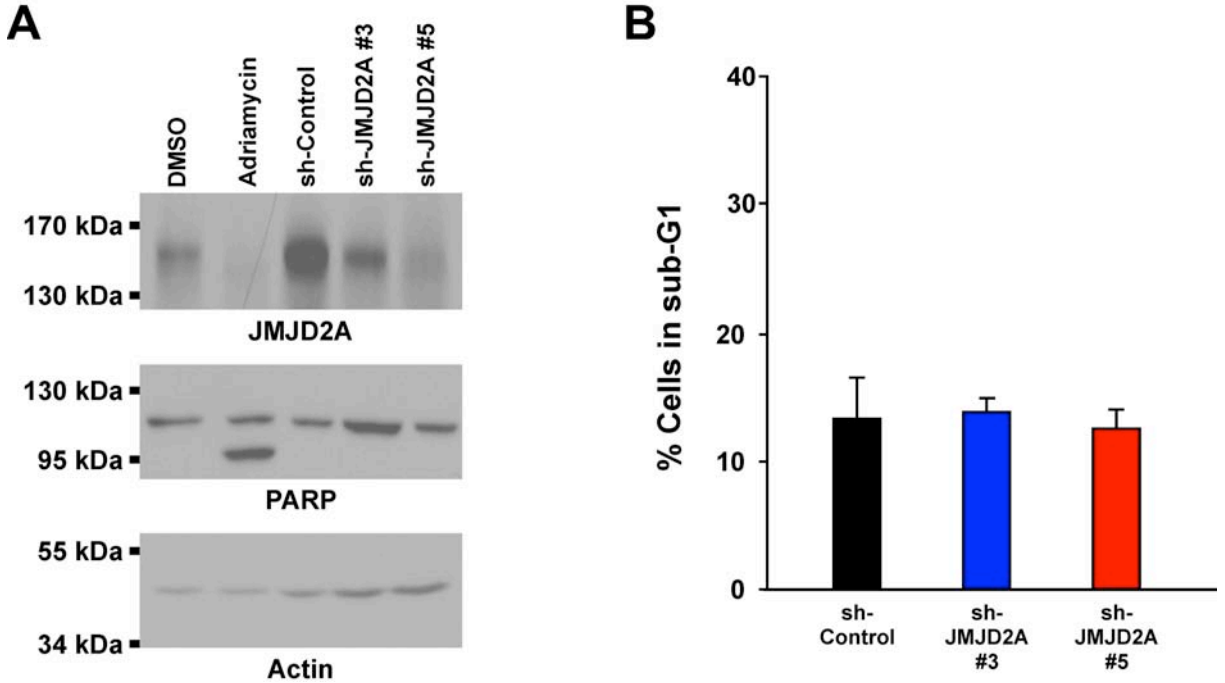
Supplemental Figure 9. Impact of JMJD2A on androgen-dependent proliferation and regulation of LNCaP cell growth by JMJD2B and JMJD2C.

(**A**) Downregulation of JMJD2A in LNCaP cells grown in phenol red-free media supplemented with charcoal-stripped serum either in the absence or presence of 10 nM mibolerone, a synthetic androgen receptor agonist. Western blotting shows JMJD2A, actin and PMEPA1 levels, the latter encoded by an androgen-inducible gene. Increased PMEPA1 expression serves as an indicator for the efficiency of induction with mibolerone.

(**B**) Corresponding growth measurement with the PrestoBlue fluorescence cell viability kit (Invitrogen). Shown are averages with standard deviations (n = 4). *, $P < 0.001$ (Student's t-test) compared to respective sh-Control.

(**C**) Downregulation of JMJD2B in LNCaP cells with two different shRNAs targeting the sequences 5'-GGTGTCAGGTGCCTGTATC-3' (#1) and 5'-GTGCTGCCTGCAGGTCCAT-3' (#2). Growth was measured with the PrestoBlue fluorescence cell viability kit (Invitrogen). Western blots show the degree of JMJD2B and actin expression. Averages (n = 3) with standard deviations are shown. $P < 0.001$ (Student's t-test) for differences between fluorescence measured with sh-Control *versus* the JMJD2B shRNAs at day 7.

(**D**) Analogous for JMJD2C. JMJD2C shRNA #2 and #3 target the sequences 5'-GCGATGACTGTGAAGGAGT-3' and 5'-CATCAGTGGCAGAGAGTAA-3', respectively.

10

Supplemental Figure 10. No impact of JMJD2A downregulation on apoptosis in LNCaP prostate cancer cells.
(**A**) LNCaP cells were treated with either DMSO or 2 µM Adriamycin (dissolved in DMSO) for 48 h or alternatively with indicated shRNAs. Shown are western blots revealing JMJD2A, Poly (ADP ribose) polymerase (PARP) and actin levels. The DNA damaging agent Adriamycin induces apoptosis as evidenced by cleavage of PARP and thus serves as a positive control in this experiment.
(**B**) LNCaP cells treated with indicated shRNAs were subjected to flow cytometry and cells in sub-G1/G0 phases determined. Shown are averages with standard deviations (n = 3).
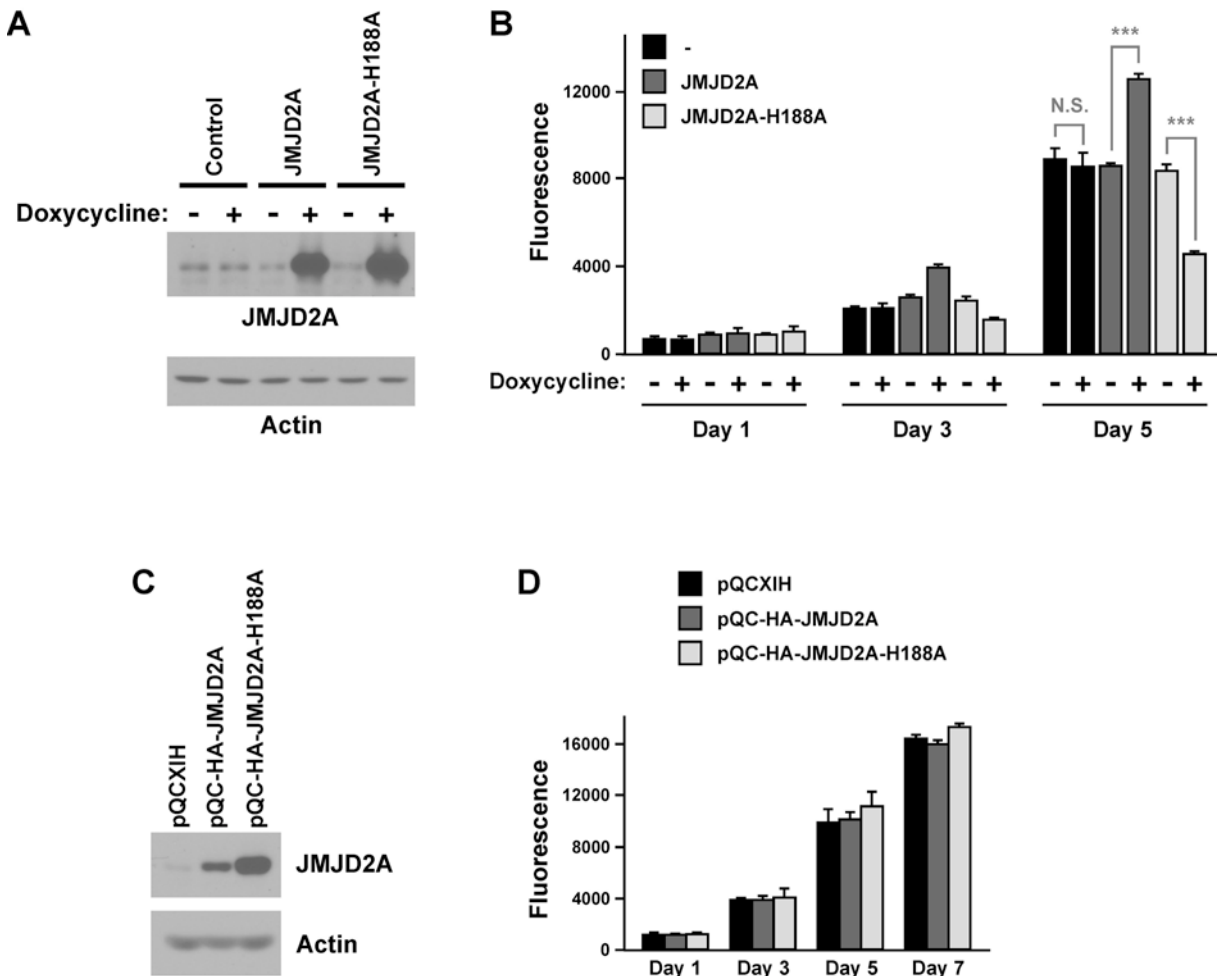
Supplemental Figure 11. Impact of JMJD2A overexpression on LNCaP and BPH-1 cell growth.
(**A**) Doxycycline-inducible stable LNCaP cells were treated with 0.25 µg/ml doxycycline for 96 h and levels of wild-type and H188A JMJD2A determined by western blotting.
(**B**) Corresponding growth measurement with the PrestoBlue fluorescence cell viability kit (Invitrogen). Shown are averages with standard deviations (n = 3). ***, $P < 0.0001$ (Student's t-test).
(**C**) Retrovirus encoding HA-tagged JMJD2A or its H188A mutant was utilized to infect normal BPH-1 cells. pQCXIH refers to the empty retroviral vector. Cells were then selected with 200 µg/ml Hygromycin B and protein extracts prepared. Expression of JMJD2A and actin was assessed by western blotting.
(**D**) Corresponding growth measurement with the PrestoBlue fluorescence cell viability kit (Invitrogen). Shown are averages with standard deviations (n = 4).
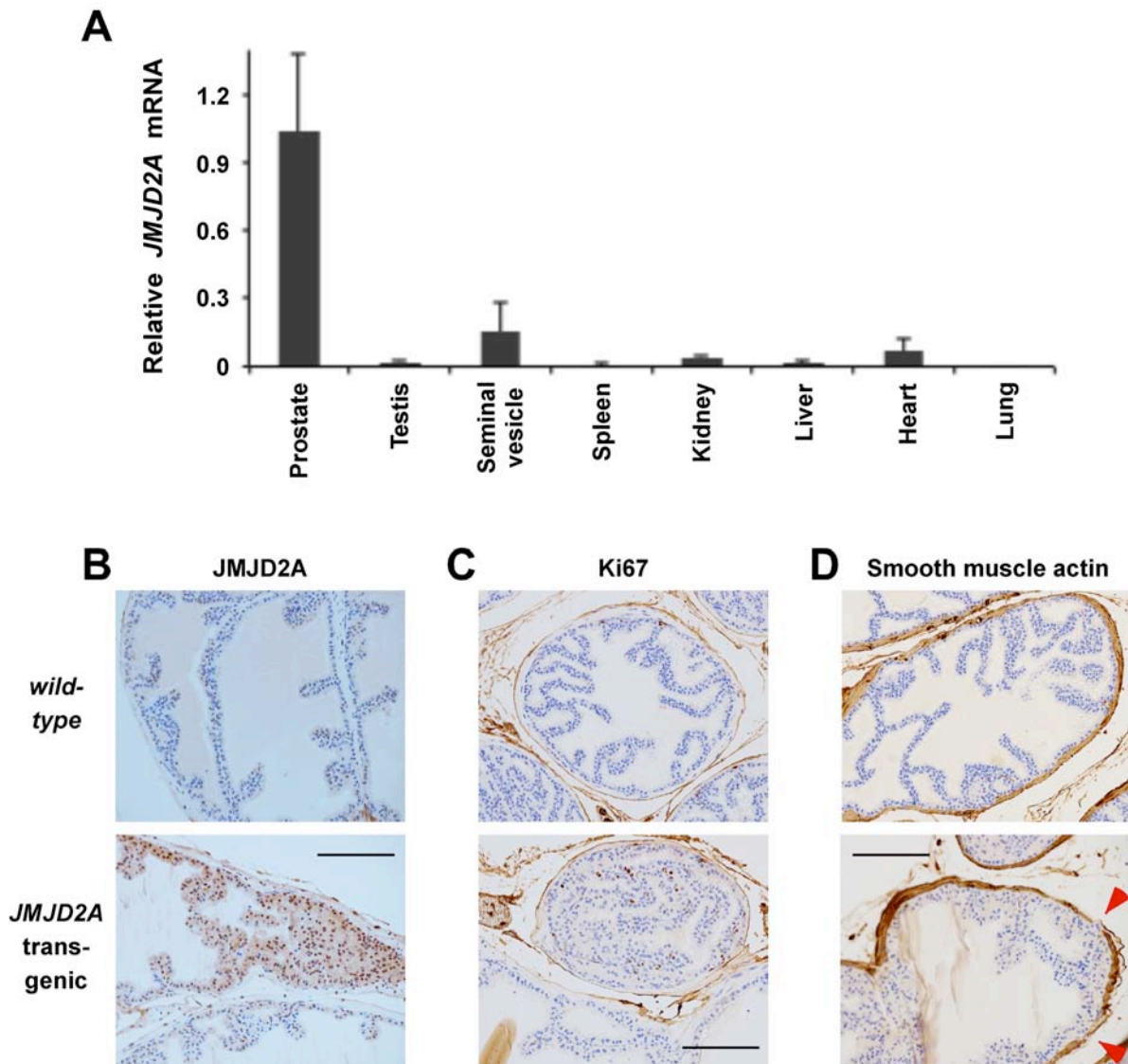
Supplemental Figure 12. Expression of the human *JMJD2A* transgene in mouse organs.
(**A**) RNA was isolated from various organs of a transgenic *JMJD2A* mouse and employed for reverse transcription with pd(N)$_6$ random primers. Performing nested PCR (1st PCR as a conventional PCR; 2nd PCR as a real-time PCR using SYBR green), the mRNA for human *JMJD2A* was quantitated and normalized to *GAPDH* levels. Primers used for the 1st PCR were J2A-Flag-1 (5'-CTCCGGATCGCCATGGCTGACTAC-3') and JMJD2A-297-rev (5'-CTTGCGGAACTCTCGAACAGTCATGG-3'). In the 2nd PCR, primers were J2A-Flag-2 (5'-GACGACAAGGGATCCGCTTCTGAG-3') and JMJD2A-255-rev (5'-GTACTGAGTAAAGAGGCCAGACTGC-3'), which will result into a 267 bp product.
(**B**) Example of JMJD2A immunohistochemical staining in the prostate of a wild-type or *JMJD2A* transgenic mouse. Scale bar = 0.1 mm.
(**C**) Likewise, staining for Ki67.
(**D**) Analogous, staining for smooth muscle actin. Arrows indicate discontinuities of the fibromuscular layer surrounding the ducts.

13
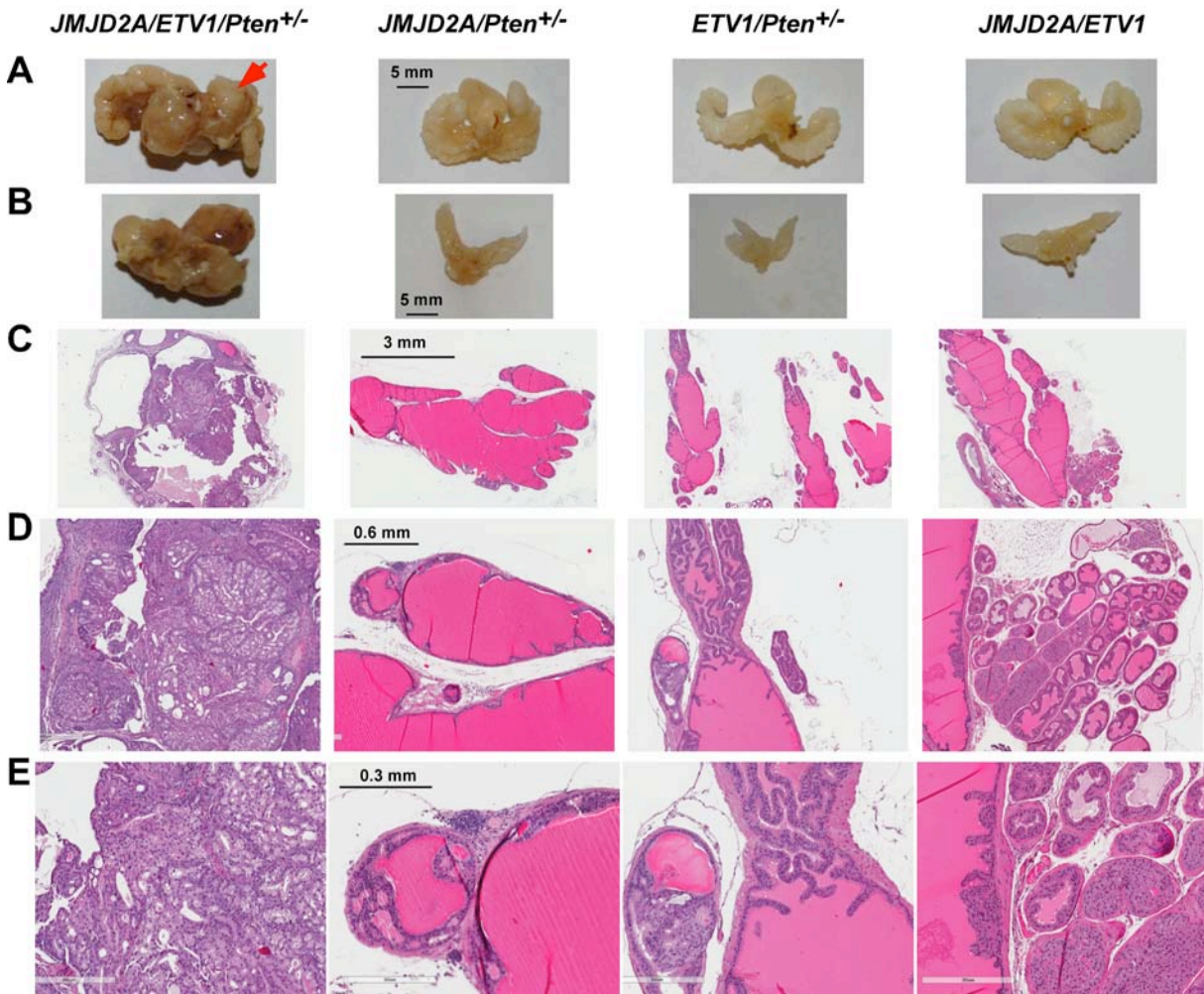
Supplemental Figure 13. Genetically engineered compound mice.
(**A**) Prostates with bladder and seminal vesicles. The *JMJD2A/ETV1/Pten*^{+/-} mouse analyzed here is the same as in Figure 4C, but here the upper neoplastic mass (marked by a red arrow) was examined.
(**B**) As above after removal of bladder and seminal vesicles.
(**C-E**) Corresponding hematoxylin/eosin stains at increasing magnification.

A

| Upstream Regulator	Predicted Activation State	Activation z-score	*P* value	Target molecules in dataset
VEGF	Inhibited	-2.96	3.42E-4	FOXN2, HMMR, ITGA6, ITGB3BP, MAD2L1, PLK4, PRKAA1, SMAD5 SMC2
HGF	Inhibited	-2.578	8.70E-4	FOXN2, HMMR, ITGA6, ITGB3BP, KRT18, MAD2L1, PLK4, PRKAA1, SMAD5, SMC2
TP53	Activated	2.147	3.57E-3	ACADVL, CTSD, CTSF, CTSH, CYB5R3, HMGB1, HMMR, IDH3G, KRT18, MAD2L1, NOL3, PBK, PMEPA1, SMC2, SUMO1, UBA1

B

|	sh-JMJD2A	sh-ETV1	Function
PRKACB	-2.48	-1.85	cAMP-dependent protein kinase
SLC39A8	-2.22	-1.63	solute carrier/zinc transporter
YAP1	-2.14	-1.82	transcriptional cofactor
PLIN5	-2.07	-1.83	coat protein for lipid storage droplets
HMMR	-2.00	-1.94	hyaluron-mediated motility receptor
....	.....	.....	....
DPP7	1.84	2.04	dipeptidyl-peptidase
NUDT16L1	1.91	1.85	syndecan-4 binding adaptor protein
HIST3H2A	1.99	1.64	histone
PMEPA1	2.15	1.58	SMAD interacting protein
GPAA1	2.17	1.51	GPI anchor attachment

Supplemental Figure 14. Microarray analyses.
(**A**) Ingenuity systems analysis done on our microarray data. Shown is how upstream regulators were affected upon treatment with ETV1 and JMJD2A shRNAs. Accordingly, VEGF and HGF signaling are predicted to be stimulated when ETV1/JMJD2A are overexpressed, whereas TP53-triggered activity would be downregulated.
(**B**) Top five JMJD2A target genes (either repressed or upregulated) that have a known/predicted function. Presented fold-expression changes are averages observed with two different JMJD2A or ETV1 shRNAs.
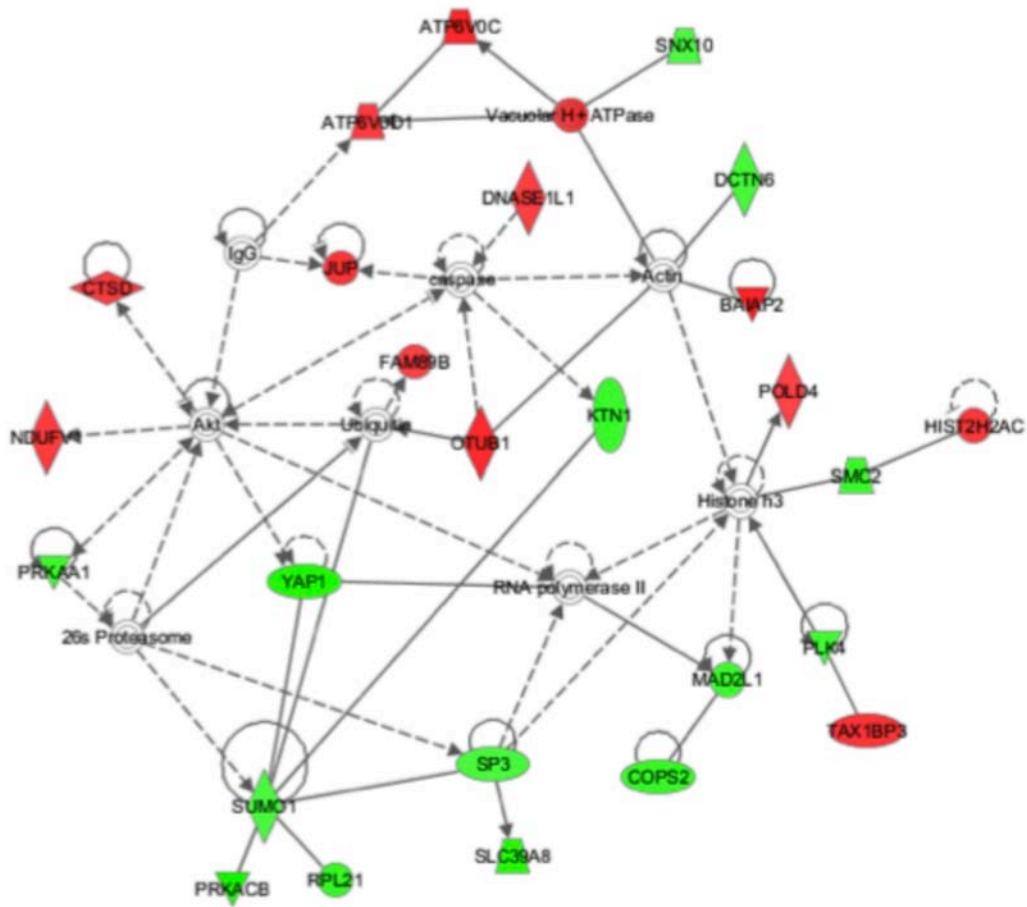
Supplemental Figure 15. Shared network containing *YAP1*.
Ingenuity pathway analysis uncovering a network shared between ETV1 and JMJD2A downregulation. Green color denotes downregulation, red color upregulation.
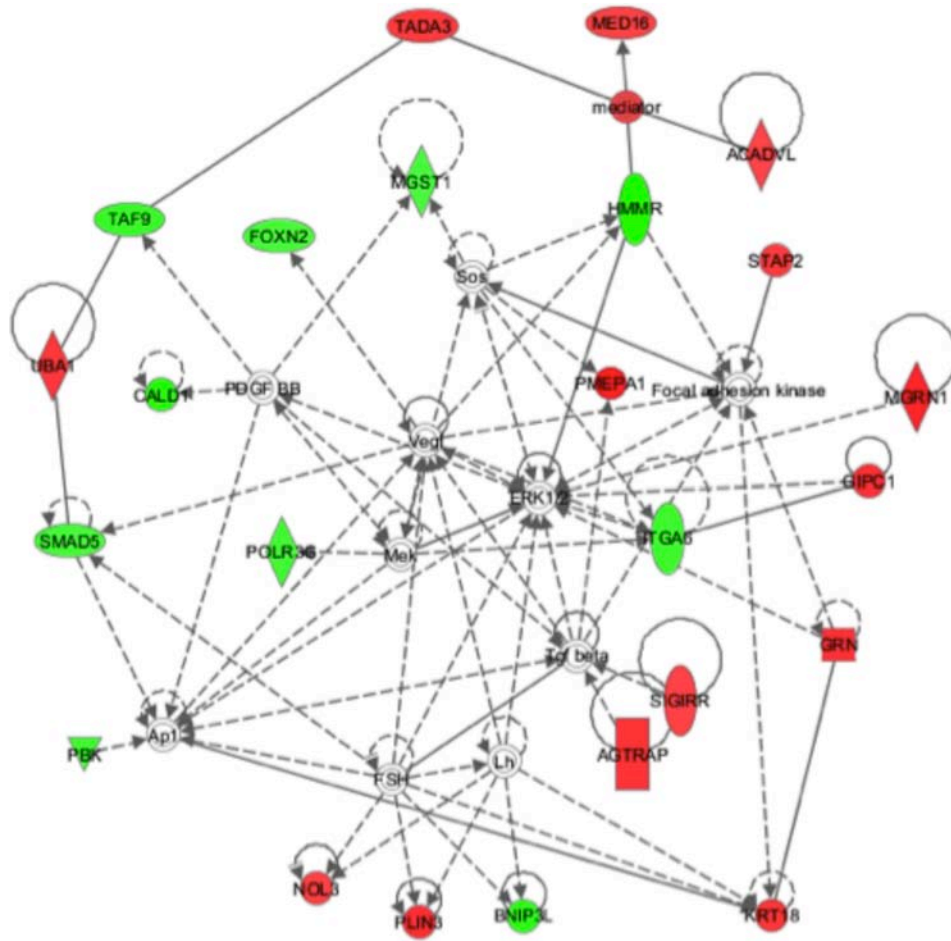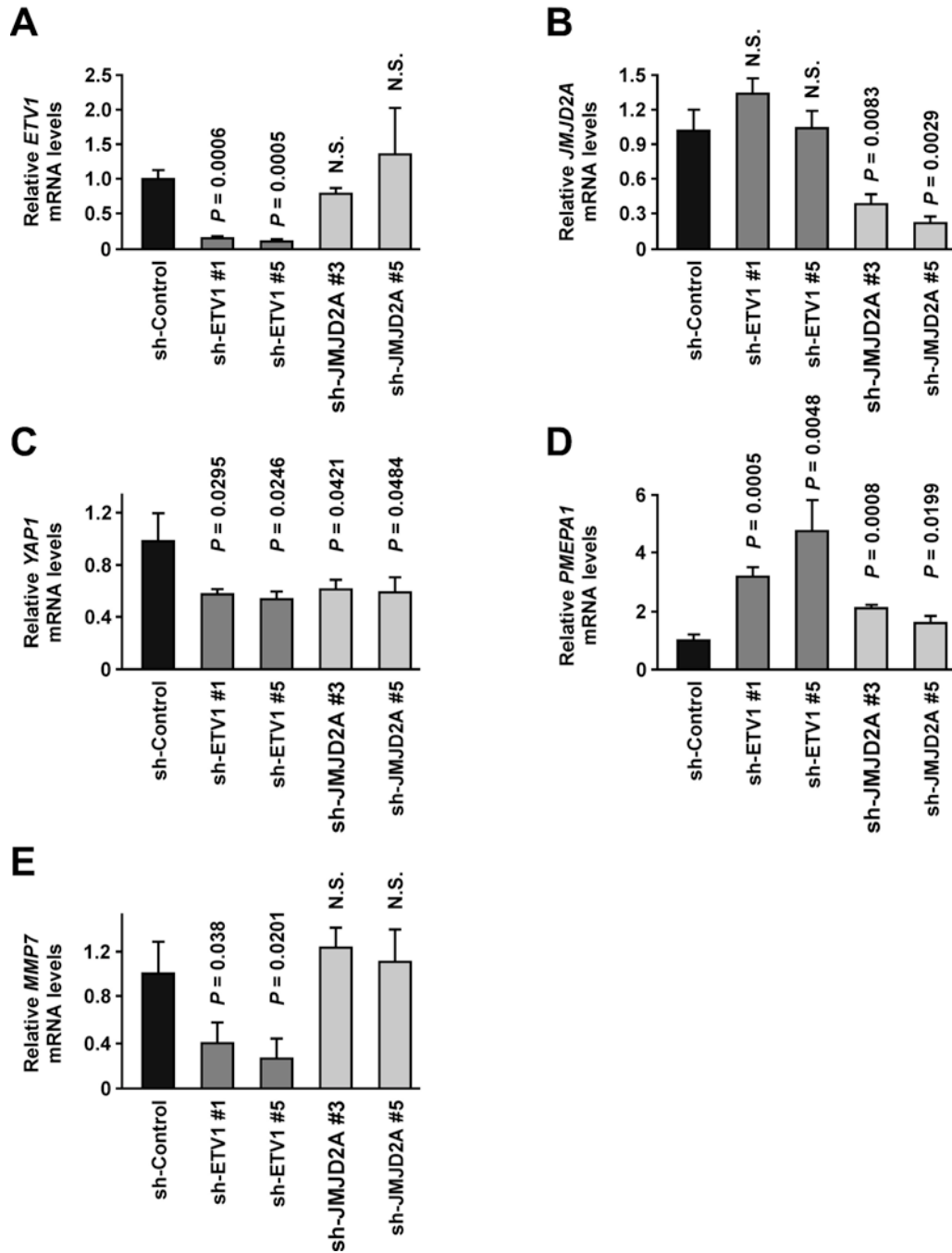
**Supplemental Figure 16. Shared network containing *PMEPA1*.**
Ingenuity pathway analysis uncovering a network shared between ETV1 and JMJD2A downregulation. Green color denotes downregulation, red color upregulation.

Supplemental Figure 17. Quantitative RT-PCR for JMJD2A and ETV1 target gene expression in LNCaP cells (corresponding to Figure 5B).
(**A**) *ETV1* mRNA levels were determined using iQ SYBR Green Supermix and the MiniOpticon real-time PCR system (BioRad). Levels of *ETV1* mRNA were normalized to those of *GAPDH*. Shown are averages with standard deviations (n = 3). Statistical significance was determined with Student's t-test. N. S., not significantly different.
(**B-F**) Similar for *JMJD2A*, *YAP1*, *PMEPA1* and *MMP7*, respectively.
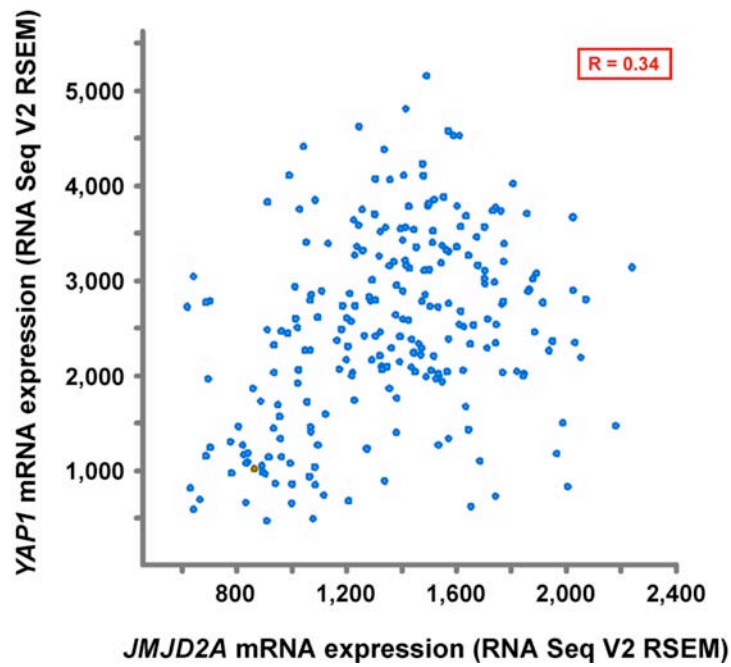
Supplemental Figure 18. Expression correlation between *YAP1* and *JMJD2A*.
Correlation between *YAP1* and *JMJD2A* mRNA levels in human prostate adenocarcinomas. Provisional data from *The Cancer Genome Atlas* (n = 236). R = 0.34 (Pearson correlation), *P* < 0.0001. Analysis was done through the cBioPortal website (www.cbioportal.org).
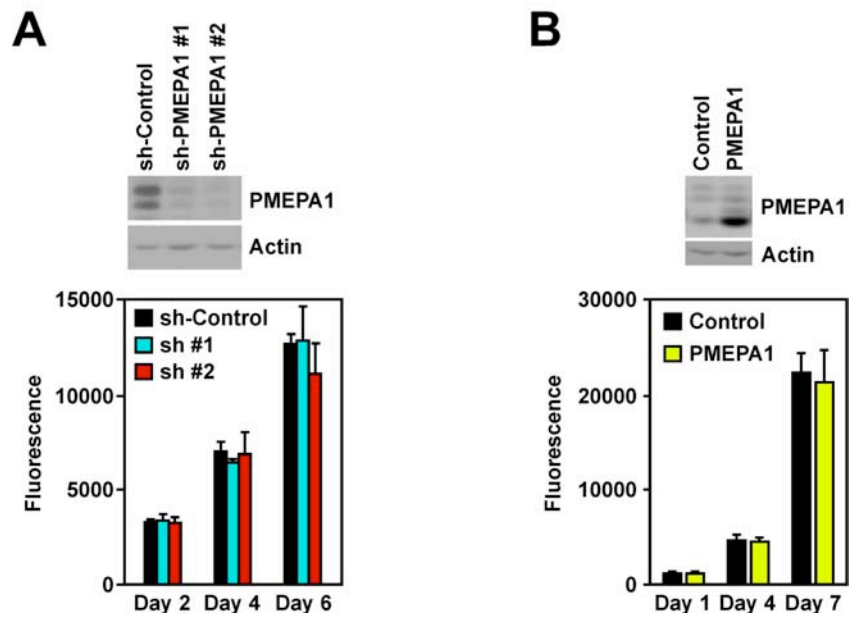
Supplemental Figure 19. No impact of PMEPA1 on LNCaP cell growth.
(**A**) Influence of PMEPA1 downregulation with two different shRNAs on LNCaP cell growth. Shown are averages (n = 3) with standard deviations and western blots for PMEPA1 and actin protein expression. PMEPA1 shRNA #1 targets the sequence 5'-GAGTAAAGCAGTTGAGCAA-3', while PMEPA1 shRNA #2 targets 5'-GGAGCAAAGAGAAGGATAA-3'.
(**B**) Likewise, retroviral overexpression of PMEPA1 or pQCXIH empty vector control.

A

kDa — Vector, JMJD2A, JMJD2A-H188A, JMJD2B, JMJD2B-H189A/E191Q, JMJD2C, JMJD2C-H190A, JMJD2D, JMJD2D-H192A

170
130
95
55

Flag Blot

43

Actin Blot
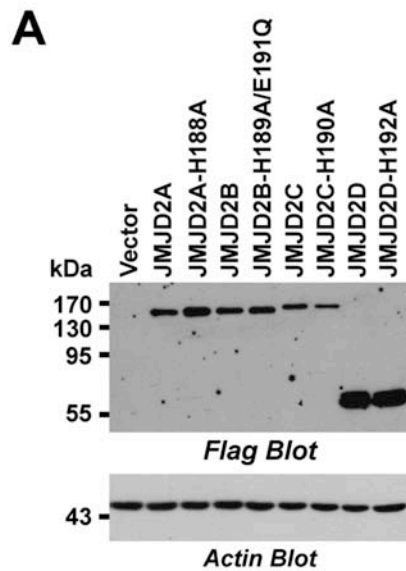
B

```
-390  CGGAGCGGAAGAACTTCCTGCAGCCAAGGGCGCCCGCGTTCTCCGCAGACACCACAGTTCGGACC
-325  CGGATTGGACCCATCGTTTGCGGTTCGCGGGGCAGAATACGGGGCACGCTTCGGGCCCCTGCCCG
-260  GCTGAGCGCGGGCGAAGGGCGGACCGGGCCAGGGCGAGCGGGTCACGTGCGGCCGGGAGAGGCGC
-195  CGCGGGCCGGGAGTGTGCAGGAATGTAGCAACTTGCAGCGAAAAGTTTCCCTGCGCTGCCGGCCG
-130  GGCCGCGGTGCGGGCGGGCGCGCAGAGGAAGGAAGAGCCGAGAGGAGGCGGGGCCGCGGCGGCGC
 -65  GGGCGGGCGCTTCTCCTAACTTTAGTTTTGGCGTTTGAGGCGAGTTTCTGTCTCAGTCGGGCGCA
 +1   GCCGCCGCCAGGGAAAAGAAAG
```

Supplemental Figure 20. **Comparable expression of the four JMJD2 proteins and location of ETS sites within the _YAP1_ gene promoter.**
(**A**) Equal amounts of indicated Flag-tagged JMJD2 expression plasmids were transfected into LNCaP cells and resulting protein levels assessed by anti-Flag western blotting. Actin levels served as controls.
(**B**) DNA sequence of the human _YAP1_ promoter from -390 to +22. The eight ETS core sequences (5'-GGA^A/$_T$-3', or 5'-^{T}/$_A$TCC-3' in reverse), which represent potential ETV1 binding sites, are highlighted in yellow.
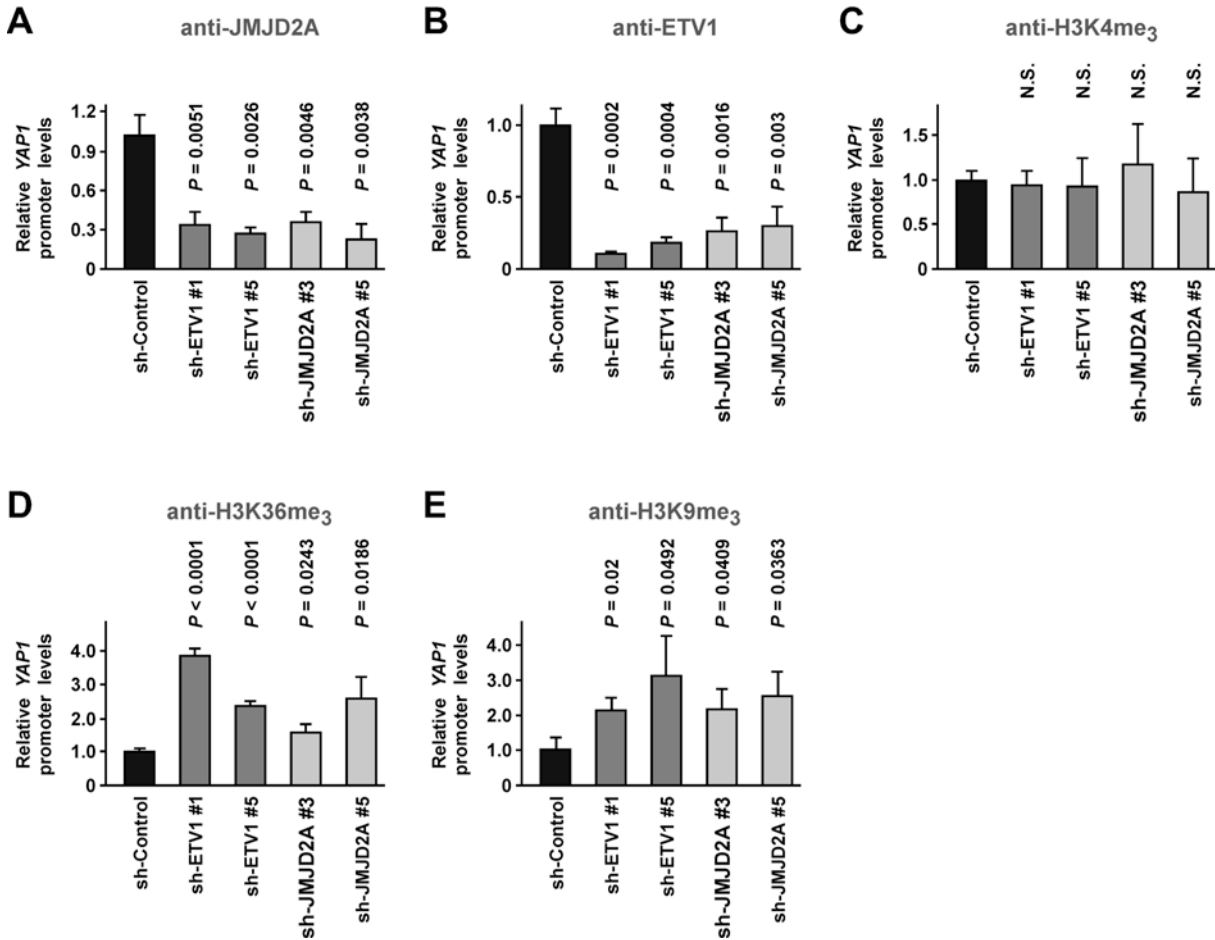
Supplemental Figure 21. Quantitative chromatin immunoprecipitation (corresponding to Figure 6D).
Quantitative PCR was performed to determine *YAP1* promoter fragment immunoprecipitation. The iQ SYBR Green Supermix and the MiniOpticon real-time PCR system (BioRad) were used. Shown are averages with standard deviations (n = 3). Statistical significance was determined with Student's t-test.
(**A**) Immunoprecipitation with anti-JMJD2A antibodies.
(**B**) Immunoprecipitation with anti-ETV1 antibodies.
(**C**) Immunoprecipitation with anti-H3K4me$_3$ antibodies.
(**D**) Immunoprecipitation with anti-H3K36me$_3$ antibodies.
(**E**) Immunoprecipitation with anti-H3K9me$_3$ antibodies.
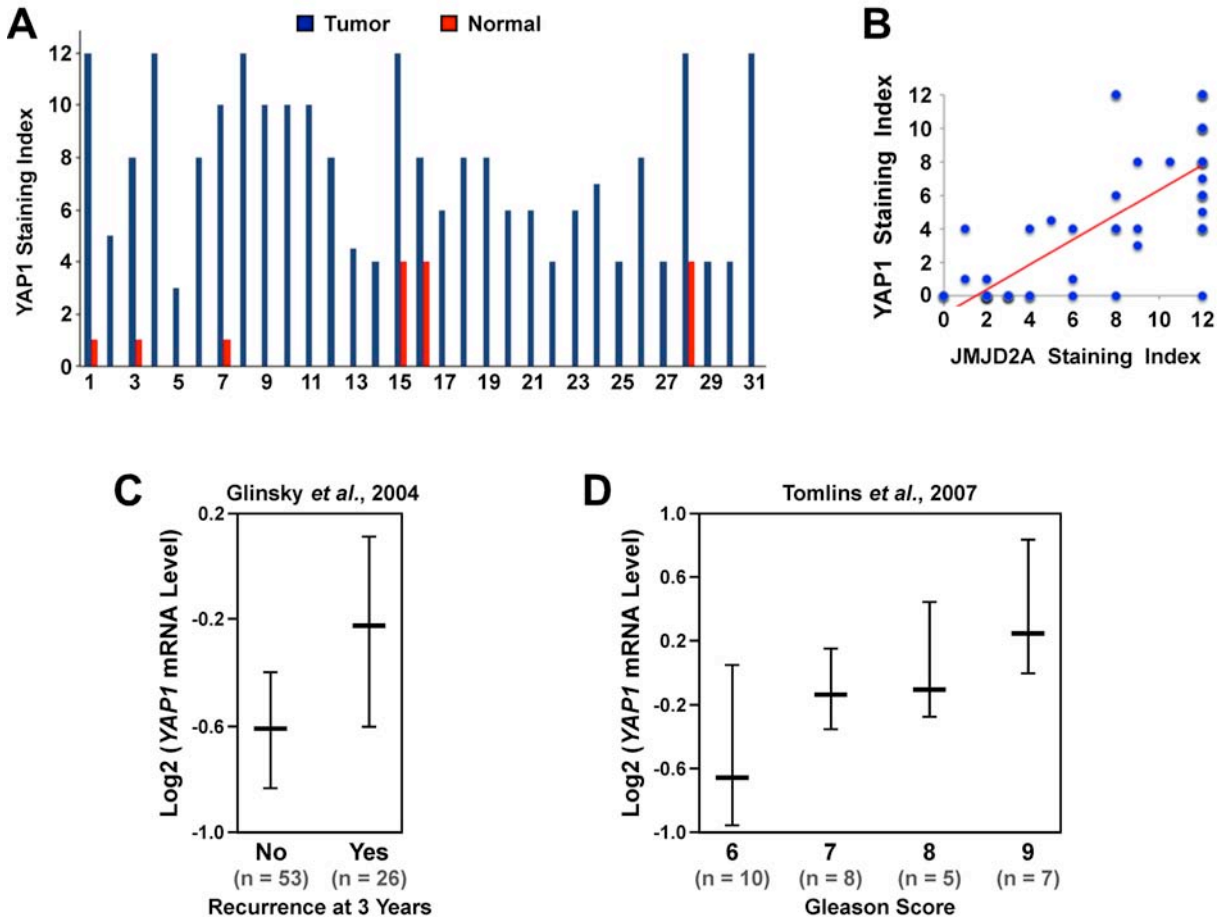
Supplemental Figure 22. Expression of YAP1 in human prostate tumors.
(**A**) Immunohistochemical nuclear staining of YAP1 in 31 matching normal and cancerous prostate tissues.
(**B**) Correlation of YAP1 and JMJD2A staining indices within the 31 human cancerous and 31 matching normal prostate tissues analyzed in this report. Trendline is marked by red color. R = 0.78, P = 3.7x10^{-14}.
(**C**) Correlation of *YAP1* mRNA levels with tumor recurrence three years after radical prostatectomy; P = 0.001 (Student's t-test). Shown are log2-transformed mRNA levels with the median and the 25 to 75 percentile range. Data were derived from a published microarray experiment (Glinsky *et al*, 2004) and analyzed with Oncomine (www.oncomine.org).
(**D**) Correlation of *YAP1* mRNA levels with Gleason score; P = 0.004 (Student's t-test). Data were derived from a published microarray experiment (Tomlins *et al*, 2007) and analyzed with Oncomine.
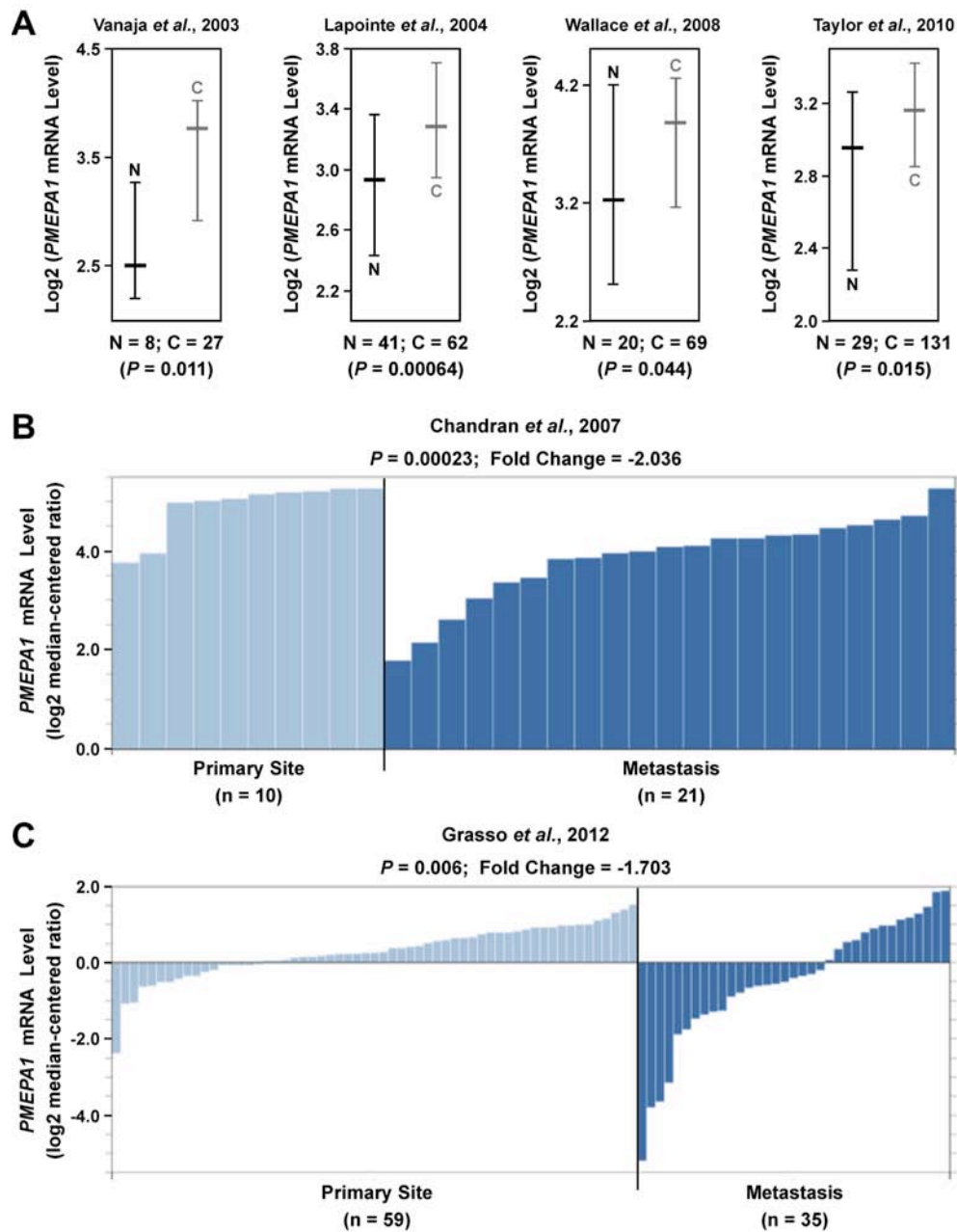
Supplemental Figure 23. Expression of *PMEPA1* in human prostate tumors.
(**A**) Expression of *PMEPA1* mRNA in normal prostates ("N") and prostate carcinomas ("C"). Numbers of analyzed specimens (both for "N" and "C") are indicated below the graphs. Shown are log2-transformed mRNA levels with the median and the 25 to 75 percentile range. Statistical significance was determined with Student's t-test. Published microarray data (Vanaja *et al*, 2003; Lapointe *et al*, 2004; Wallace *et al*, 2008; Taylor *et al*, 2010) were analyzed with Oncomine (www.oncomine.org).
(**B**) Downregulation of *PMEPA1* mRNA levels at metastatic sites compared to the primary prostate tumor was evaluated with Student's t-test. Each bar represents one patient. Data were derived from a published microarray experiment (Chandran *et al*, 2007) and analyzed with Oncomine.
(**C**) Likewise with data from another published microarray experiment (Grasso *et al*, 2012).

LEGENDS TO SUPPLEMENTAL TABLES

Supplemental Table 1.   Transgenic *JMJD2A* Mice.

Transgenic *JMJD2A* mice established from founders 502 and 519 were aged for 5, 9-10 or 13 months and pathologically analyzed. The PIN grade is defined as the highest one found in the anterior and ventral prostate lobes. No abnormality was assigned a PIN grade of 0 and hyperplasia a PIN grade of 0.5. In addition, the diagnoses of the four founder mice at 12 or 13 months of age are presented.

Supplemental Table 2.   JMJD2A Target Genes.

Genes that were up- or downregulated by more than 1.4-fold upon expression of each JMJD2A shRNA (#3 or #5) in LNCaP cells. Microarray signal intensities for treatment with control and the two JMJD2A shRNAs are also presented.

Supplemental Table 3.   ETV1 Target Genes.

Genes that were up- or downregulated by more than 1.4-fold upon expression of each ETV1 shRNA (#1 or #5) in LNCaP cells. Microarray signal intensities for treatment with control and the two ETV1 shRNAs are also presented.

Supplemental Table 4.   Shared Target Genes.

Compilation of shared target genes encompassed in both Supplemental Table 2 and Supplemental Table 3. Genes were ranked in ascending order with regard to their averaged response to the two JMJD2A shRNAs.

SUPPLEMENTAL REFERENCES

Arredouani MS, Lu B, Bhasin M, Eljanne M, Yue W, Mosquera JM, Bubley GJ, Li V, Rubin MA, Libermann TA, Sanda MG (2009) Identification of the transcription factor single-minded homologue 2 as a potential biomarker and immunotherapy target in prostate cancer. *Clin Cancer Res* 15: 5794-5802

Bosc DG, Goueli BS, Janknecht R (2001) HER2/Neu-mediated activation of the ETS transcription factor ER81 and its target gene MMP-1. *Oncogene* 20: 6215-6224

Chandran UR, Ma C, Dhir R, Bisceglia M, Lyons-Weiler M, Liang W, Michalopoulos G, Becich M, Monzon FA (2007) Gene expression profiles of prostate cancer reveal involvement of multiple molecular pathways in the metastatic process. *BMC Cancer* 7: 64

Glinsky GV, Glinskii AB, Stephenson AJ, Hoffman RM, Gerald WL (2004) Gene expression profiling predicts clinical outcome of prostate cancer. *J Clin Invest* 113: 913-923

Grasso CS, Wu YM, Robinson DR, Cao X, Dhanasekaran SM, Khan AP, Quist MJ, Jing X, Lonigro RJ, Brenner JC, Asangani IA, Ateeq B, Chun SY, Siddiqui J, Sam L, Anstett M, Mehra R, Prensner JR, Palanisamy N, Ryslik GA *et al* (2012) The mutational landscape of lethal castration-resistant prostate cancer. *Nature* 487: 239-243

Lapointe J, Li C, Higgins JP, van de Rijn M, Bair E, Montgomery K, Ferrari M, Egevad L, Rayford W, Bergerheim U, Ekman P, DeMarzo AM, Tibshirani R, Botstein D, Brown PO, Brooks JD, Pollack JR (2004) Gene expression profiling identifies clinically relevant subtypes of prostate cancer. *Proc Natl Acad Sci USA* 101: 811-816

Liu P, Ramachandran S, Ali Seyed M, Scharer CD, Laycock N, Dalton WB, Williams H, Karanam S, Datta MW, Jaye DL, Moreno CS (2006) Sex-determining region Y box 4 is a transforming oncogene in human prostate cancer cells. *Cancer Res* 66: 4011-4019

Singh D, Febbo PG, Ross K, Jackson DG, Manola J, Ladd C, Tamayo P, Renshaw AA, D'Amico AV, Richie JP, Lander ES, Loda M, Kantoff PW, Golub TR, Sellers WR (2002) Gene expression correlates of clinical prostate cancer behavior. *Cancer Cell* 1: 203-209

Taylor BS, Schultz N, Hieronymus H, Gopalan A, Xiao Y, Carver BS, Arora VK, Kaushik P, Cerami E, Reva B, Antipin Y, Mitsiades N, Landers T, Dolgalev I, Major JE, Wilson M, Socci ND, Lash AE, Heguy A, Eastham JA *et al* (2010) Integrative genomic profiling of human prostate cancer. *Cancer Cell* 18: 11-22

Tomlins SA, Mehra R, Rhodes DR, Cao X, Wang L, Dhanasekaran SM, Kalyana-Sundaram S, Wei JT, Rubin MA, Pienta KJ, Shah RB, Chinnaiyan AM (2007) Integrative molecular concept modeling of prostate cancer progression. *Nat Genet* 39: 41-51

Vanaja DK, Cheville JC, Iturria SJ, Young CY (2003) Transcriptional silencing of zinc finger protein 185 identified by expression profiling is associated with prostate cancer progression. *Cancer Res* 63: 3877-3882

Varambally S, Yu J, Laxman B, Rhodes DR, Mehra R, Tomlins SA, Shah RB, Chandran U, Monzon FA, Becich MJ, Wei JT, Pienta KJ, Ghosh D, Rubin MA, Chinnaiyan AM (2005) Integrative genomic and proteomic analysis of prostate cancer reveals signatures of metastatic progression. *Cancer Cell* 8: 393-406

Wallace TA, Prueitt RL, Yi M, Howe TM, Gillespie JW, Yfantis HG, Stephens RM, Caporaso NE, Loffredo CA, Ambs S (2008) Tumor immunobiological differences in prostate cancer between African-American and European-American men. *Cancer Res* 68: 927-936

Welsh JB, Sapinoso LM, Su AI, Kern SG, Wang-Rodriguez J, Moskaluk CA, Frierson HF, Jr., Hampton GM (2001) Analysis of gene expression identifies candidate markers and pharmacological targets in prostate cancer. *Cancer Res* 61: 5974-5978

Yu YP, Landsittel D, Jing L, Nelson J, Ren B, Liu L, McDonald C, Thomas R, Dhir R, Finkelstein S, Michalopoulos G, Becich M, Luo JH (2004) Gene expression alterations in prostate cancer predicting tumor aggression and preceding development of malignancy. *J Clin Oncol* 22: 2790-2799